Collective excitation of ^{101}Pd following (heavy ion, xn) reactions*

P. C. Simms, G. J. Smith†, F. A. Rickey, J. A. Grau, J. R. Tesmer‡, and R. M. Steffen
Tandem Accelerator Laboratory, Purdue University, Lafayette, Indiana 47907
(Received 23 October 1973)

States excited by the ^{99}Ru($\alpha, 2n\gamma$)^{101}Pd, ^{88}Sr(^{16}O, $3n\gamma$)^{101}Pd, and ^{92}Zr(^{12}C, $3n\gamma$)^{101}Pd reactions have been studied by measuring the γ-ray yield as a function of incident projectile energy, γ-γ coincidences, γ-ray angular distributions, and γ-ray linear polarizations. Three intense γ-ray cascades were observed. These cascades are produced by quasirotational bands built on the $5/2^+$, $7/2^+$, and $11/2^-$ intrinsic states of the nucleus. A decay scheme is given which includes states with energy up to 6488 keV and angular momentum up to 35/2. The quasirotational bands seen in ^{101}Pd are similar to the bands in the adjacent even-even nuclei which suggests that this odd-A nucleus can be described as a particle decoupled from an even-even core. A cascade of seven γ rays in ^{102}Rh was also observed following the ^{92}Zr(^{12}C, $p\ n$)^{102}Rh reaction.

[NUCLEAR REACTION ^{99}Ru($\alpha, 2n\gamma$), E=16–24 MeV; ^{92}Zr(^{12}C, $3n\gamma$), E=45–56 MeV; ^{88}Sr(^{16}O, $3n\gamma$), E=56–64 MeV; measured $\sigma(E)\gamma$, γ-γ coin, $\sigma(\theta)\gamma$, linear P; deduced decay scheme, J, π.]

I. INTRODUCTION

In recent experiments[1-3] using (heavy ion, xn) reactions strong γ-ray cascades were found in the neutron deficient, even-even nuclei ^{100}Pd, ^{102}Pd, and ^{104}Pd. Similar cascades had previously been observed[4] in even-even Ru and Mo nuclei. The sets of states involved in these cascades are reminiscent of ground-state rotational bands in strongly deformed nuclei in that they exhibit a $0^+, 2^+, 4^+, \ldots$ spin sequence; however, the rotational $I(I+1)$ energy spacings are not followed. Instead the energy spacings are in good agreement with the variable moment of inertia (VMI) interpretation[5] of a "soft" nucleus with a small deformation which increases with increasing I. Since the states are apparently collective, it is natural to think of them as being members of bands which are "quasirotational." That is, the mode of excitation can be interpreted as a rotation even though the nuclear deformation is neither large nor rigid.

It is interesting to look for similar collective excitations in odd-A nuclei. No clear-cut evidence for quasirotational bands was found in a series of Mo and Ru nuclei which were studied by Lederer, Jaklevic, and Hollander.[6] In a preliminary report[7] we have described three well-developed quasirotational bands in ^{101}Pd built on the $\frac{5}{2}^+$, $\frac{7}{2}^+$, and $\frac{11}{2}^-$ intrinsic states. These band heads have been shown[8] to be relatively pure single-particle states. The similarity between the ground state ($\frac{5}{2}^+$) band in ^{101}Pd and the quasirotational ground state band in ^{100}Pd[1] suggest that ^{101}Pd can be described as a particle coupled to a ^{100}Pd core. Since there is a difference in angular momentum of 2 units between successive states in the bands, it is evident that the particle is not strongly coupled to the core.

This paper presents an extensive report on our ^{101}Pd experiments and results. Additional data and analysis have added several new states to the bands previously reported,[7] have removed uncertainties in several angular momenta assignments, and have set better limits on the intensity of transitions between the bands. Two alternate approaches to particle-core coupling will be considered in Sec. IV.

We have performed in-beam γ-ray experiments with the following three reactions: ^{99}Ru($\alpha, 2n$)-^{101}Pd, ^{92}Zr(^{12}C, $3n$)^{101}Pd, and ^{88}Sr(^{16}O, $3n$)^{101}Pd. The experiments included the observation of γ-ray yields as a function of incident projectile energy (excitation functions), γ-γ coincidences, γ-ray angular distributions, and γ-ray linear polarizations. The excitation functions were used to assign the intense γ rays to a particular isotope. Then the coincidence measurements were used to assign other γ rays to the identified nuclei and to determine the decay scheme. The γ-ray angular distributions and linear polarization measurements were used to determine the multipole character of the γ rays and to assign angular momenta to the nuclear states.

II. EXPERIMENTAL TECHNIQUE

A. General

The heavy ions were accelerated in the Purdue

FN tandem Van de Graaff accelerator. The ^{99}Ru targets were prepared by evaporating metallic Ru (98% enriched) from a cold crucible and condensing the Ru as a thin film (~100 μg/cm^2) on a 70-μg/cm^2 carbon backing to make the ^{99}Ru target. The enriched ^{88}Sr (99%) was reduced from SrO by heating a SrO-Th mixture in vacuum. The ^{88}Sr targets were made by evaporating a thin film (~200 μg/cm^2) of Sr metal onto a Au backing (~10 mg/cm^2). A Au covering film (~2 mg/cm^2) was evaporated on top of the Sr to protect it from oxidation when the target was exposed to air. The ^{92}Zr was obtained from Oak Ridge National Laboratory as an enriched (96%), rolled foil of 3.6-mg/cm^2 thickness. Since the Ru and Sr targets were relatively thin, the target backings produced a significant amount of background radiation. The Zr targets were superior in this respect since they were relatively thick and had no backings.

Several Ge(Li) detectors were used in the experiments. The energy resolution varied from 2.1 to 2.7 keV. Seven well-known γ rays from 121.97 to 1332.48 keV were used to determine the four coefficients of a third power polynomial expression for the γ-ray energy calibration curve. The rms deviation of the calibration lines from the polynomial was 0.04 keV. The calibration sources were present when the energy of the ^{101}Pd γ rays was measured, so the results were not affected by gain shifts.

Two small chambers were used in the experiments. The angular distribution chamber differed from the general purpose chamber in that it did not have an exit pipe so the detector could be positioned on both sides of the beam line and at 0°. When this chamber was used, the beam was stopped by a Au foil located immediately behind the target.

B. Excitation functions

The detector was positioned at approximately 145° with respect to the beam direction so that neutron damage to the Ge(Li) detector would be minimal.

A detailed description of the procedure used to correct for dead-time and pileup losses and to normalize to unit beam current has been given previously.[3] A pulser, which is driven by the digital output of the current integrator, was connected to the system such that it suffered the same losses as the detector. The area of the pulser peak in the γ-ray spectrum was used to correct and normalize the area of all the γ-ray peaks. The correction system has been shown to have an accuracy of better than 0.5%. The singles counting rate was typically 15×10^3 counts/sec and the counting rate losses were approximately 30%.

C. Coincidence measurements

The two Ge(Li) detectors were located at −90 and +145° with respect to the beam axis. The coincidence electronic system[3] recorded true and chance coincidences simultaneously. A number of time pickoff devices were used with the Ge(Li) detectors. By far the best results were obtained with a pair of "snap-off" discriminators (Elscint model STD-N-1). (There is one subtle point in obtaining good results with these discriminators. When the snap-off diode bias is adjusted to optimize the time resolution, the part of the case which covers the foil side of the printed circuit board *must* be left in place. Removing this cover has a very adverse effect on the performance of the instrument).

The coincidence system had the following typical performance characteristics: coincidence resolving time $2\tau = 50$ nsec, true-to-chance ratio $T/C = 30:1$. Coincidence rates were approximately 10^3 counts/sec. (A coincidence rate of 10^3 might seem high with a singles rate of 15×10^3, but it occurs because so many coincidence combinations are possible.)

The coincidence events were processed and stored by a PDP 15/40 computer. All coincidence events were stored on magnetic tape during the first phase of the experiment. At the same time a coincidence-spectrum projection was stored in core for each detector. (A projection has all of the γ rays in one detector which were coincident with any γ ray in the other detector.) After enough data had been accumulated to determine which γ rays were present in the coincidence projections, digital windows were set to exclude those parts of the A-detector spectrum which were clearly of no interest.

Normalization of the coincidence data was important so that it could be used to help establish the relative intensity of the transitions. When the storage tapes were searched, the analog-to-digital-converter–A (ADC-A) projection was used to set digital windows on peaks and on the corresponding backgrounds. A skewed Gaussian line shape was fitted to each peak in the projection so that the fraction of the peak that was contained in the window could be computed. The product of the efficiency of the two detectors was also used to normalize the coincidence data. A spectrum of all the γ rays recorded in detector B was reconstructed in the tape search for each peak and each background window. A consistent scheme was used to look for all possible γ rays in each of these spectra. The dominant γ rays were selected from the B-ADC projection. After the major features of the decay scheme were estab-

lished, all the spectra were reexamined for weak γ rays—particularly for those emitted in crossing transitions between bands.

A number of procedures were considered before a good way was developed to record quickly and accurately the area of peaks which have poor statistics. Strong, clean peaks in the B-ADC projection were used to measure the change in the skewness and width of the peaks as a function of the energy deposited in the detector. Then these parameters were calculated and a skewed Gaussian was fitted for position and height to each peak (or suspected peak) in all spectra. For each γ ray, the area in the background spectrum was subtracted from the area in the peak spectrum.

Accurate chance-coincidence corrections, which were needed to set good limits on weak transitions, were possible because the true-to-chance coincidence ratio was good (>30:1) and the chance events were recorded simultaneously with the true events. The chance events were subtracted from the true events as the data was read from the storage tapes.

The coincidence counting rate was large, so storage tapes were filled rather quickly. It took about half as much time to read the storage tapes once as it did to take the data. Since we could reconstruct 127 2048-channel spectra simultaneously on a disk, only one pass through the storage tapes was necessary.

D. Angular distributions

The angular distribution experiment was performed with the reaction ^{92}Zr(^{12}C, $3n$)^{101}Pd at 48 MeV. A layer of Au (5 mg/cm^2) was vacuum evaporated onto the back of the Zr foil target to prevent Pd nuclei from recoiling out of the target. The nuclear lifetimes are so short that Doppler shifts would occur for ions recoiling in space, and the angular distributions would be distorted. A 2.5×10^{-2}-mm-thick Au foil was placed immediately behind the target to stop the incident beam since the angular distribution chamber does not have a beam exit line.

The beam was defined by two collimators; 2.4 and 12 mm at a distance of 0.25 and 2 m from the target, respectively. Beam centering was checked to better than 0.6% by measuring the angular distribution of γ rays from radioactivity produced in the target. As a check on alignment, the angular distributions were all fitted with the angle θ_0 between the table and the beam direction left as a free parameter. It was found to be $(-1.3\pm0.6)°$. Beam wobble during the experiment was checked with a Ge(Li) monitor detector located at −90° with respect to the beam axis. The rms deviation of the monitor detector counting rate (0.3%) was used to set a *lower limit* on the uncertainty that was assigned to all counting rates. The monitor detector was *not* used to normalize the angular distribution data, but instead it was an independent check on the normalization procedure which has been described briefly in Sec. II B and in detail in Ref. 3.

The target-to-detector distance was 6.3 cm. The geometrical correction factors coefficients were $Q_2=0.95$ and $Q_4=0.84$ for γ rays with energy above 500 keV. The Q_k were corrected for small changes at lower energies. The target was located at a 60° angle with respect to the beam line. The detector was positioned at nine evenly spaced angles from +90 to −30° with respect to the beam line. Three complete cycles were made with 15-min live counting periods at each angle. The rms deviation of the three repeated measurements was also used as a lower limit on the accuracy assigned to the average of the three runs.

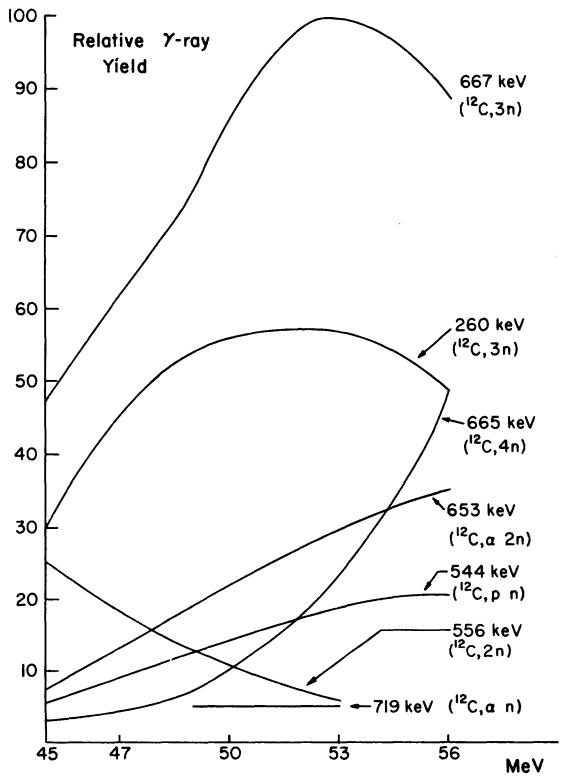

FIG. 1. γ-ray yield as a function of incident projectile energy when ^{92}Zr is bombarded with ^{12}C. The primary reaction is ^{92}Zr(^{12}C, $3n$)^{101}Pd, but a number of important competing reactions are also shown for comparison. The average energy of the projectile in the target was approximately 3 MeV lower than that shown in the figure.

E. Linear polarization

The linear-polarization measurements were performed in collaboration with Lee and Kim of John Hopkins University and Hardy of Florida International University. The polarization-spectrometer provided by Lee consists of two coaxial Ge(Li) detectors mounted in a rotating cryostat. The output signals from the two crystals were added and an event was accepted only if there was a coincidence between the two crystals. Since the probability of Compton scattering from one crystal to the other depends on the linear polarization of the incident γ ray, the coincidence counting rate depends on whether the two crystals are orientated perpendicular or parallel to the beam line. The two-crystal combination gave approximately 4-keV resolution at 1.33 MeV. Very good results were obtained for 14 ^{101}Pd γ rays after a period of 5 h with each detector counting at a rate of approximately 8×10^3 counts/sec. This experimental technique for measuring linear polarizations has been described previously.[9] The details of the present linear polarization measurement will be presented in a subsequent publication.[10]

III. RESULTS

A. Excitation function

The excitation function for the most important nuclei which were produced when ^{92}Zr was bombarded with ^{12}C are shown in Fig. 1. (The target was relatively thick so the effective energy of the projectile was approximately 3 MeV lower than indicated on the energy axis of Fig. 1.) The curves show the relative intensity of the dominant ground-state transitions as a function of incident projectile energy. Both of the strong ground-state transitions in ^{101}Pd (667 and 261 keV) are shown. In the energy range from 45 to 56 MeV the (^{12}C, $3n$)^{101}Pd reaction is clearly most probable. However the competition from (^{12}C, $2n$)^{102}Pd, (^{12}C, $4n$)^{100}Pd, (^{12}C, $\alpha\,2n$)^{98}Ru, (^{12}C, αn)^{99}Ru, and (^{12}C, pn)^{102}Rh was quite significant. Since ^{102}Pd,[3] ^{100}Pd,[1] ^{98}Ru,[4] and ^{99}Ru[6] had all been studied previously, these competing reactions were easily identified.

The assignment of the 544-keV γ ray (and a cascade which is in coincidence with it) to ^{102}Rh was more difficult because very little is known about this nucleus. It is easy to see that there is a significant difference between the excitation function for this γ ray and the ones for ^{101}Pd γ rays. It is evident that the 544-keV γ-ray excitation function does not rise as steeply as the ^{100}Pd or ^{98}Ru excitation functions. Furthermore the previous experiments[1,4,6] on these nuclei show no evidence of a 544-keV γ ray. Therefore it appears that this γ ray is emitted following a (^{12}C, $p\,xn$) reaction. Since the (^{12}C, $\alpha\,2n$) reaction has an angular-momentum and Q-value advantage over the (^{12}C, $p\,2n$) reaction, the 544 keV excitation function appears to be peaking too early to be caused by the latter process. Thus the most likely choice is that the 544-keV γ ray is produced in the reaction ^{92}Zr(^{12}C, pn)^{102}Rh. There are two independent confirmations of this assignment. When ^{92}Zr is bombarded with ^{13}C ions, the 544-keV γ ray is first seen at 53 MeV and its intensity increases dramatically as the energy is increased to 56 MeV. This energy dependence is quite reasonable for the ^{92}Zr(^{13}C, $p\,2n$)^{102}Rh reaction. Furthermore, a state has been seen[11] at 544 keV in the ^{103}Rh(p, d)^{102}Rh reaction.

Our coincidence and angular-distribution experiments were run at 48 MeV to minimize the background from competing reactions. The (^{12}C, $2n$) excitation function, which is partially shown in Fig. 1, does not rise significantly below 45 MeV. The Coulomb barrier of the target nucleus makes the total cross section drop before the $2n$ process becomes dominant over the $3n$ process. There is a significant change in the (^{12}C, $3n$) excitation function when a target with two neutrons less is used. The ^{90}Zr(^{12}C, $3n$)^{99}Pd excitation function[12] is still rising at 56 MeV, and the ^{90}Zr (^{12}C, $2n$)^{100}Pd excitation function peaks at approximately 49 MeV. The shift in the excitation function for a target with two more neutrons is not as dramatic. The ^{94}Zr(^{12}C, $3n$)^{103}Pd excitation function[13] peaks at approximately 50 MeV.

The excitation function for the ^{99}Ru(α, xn) reaction has been given previously.[3] The (α, n) reaction peaks at 18 MeV and then drops while the (α, $2n$) reaction rises to 25 MeV (and presumably higher). It is very easy to distinguish between the (α, n) and (α, $2n$) excitation functions. The distinction between the $3n$ and the other reactions was not quite clear when ^{16}O rather than ^{12}C was used as a projectile. The (^{16}O, $3n$) reaction continued to rise in the energy interval from 52 to 64 MeV. The other reactions had similar excitation functions to those shown in Fig. 1. That is, the (^{16}O, $2n$) drops in the interval from 52 to 64 MeV, the (^{16}O, p-n) has a shape very similar to the (^{16}O, $3n$), and the (^{16}O, $\alpha\,2n$) rises about twice as fast as the (^{16}O, $3n$). The (^{16}O, $4n$) first appears at 58 MeV and its yield doubles every 2 MeV up to 64 MeV.

B. Coincidence measurements

The γ rays listed in Table I are all in coincidence with several γ rays which had been uniquely

assigned to ^{101}Pd by the α, ^{12}C, and ^{16}O excitation functions. The relative γ-ray intensities for the three reactions given in columns 3, 4, and 5 were obtained by combining singles and coincidence rates. The intensity of the 667-keV γ ray has been set equal to 100 for all three reactions. We have listed uncertainties only for the ^{12}C reaction where we have complete experimental data. The sixth column gives the energy of relatively intense background γ rays which interfered with ^{101}Pd lines. The next two columns give the intensity of the background lines for the α and ^{12}C reactions. (^{16}O would be similar to ^{12}C.) The nuclei which emit the background γ rays are given in the ninth column. The last column gives the source of information for the background γ rays.

Our results for the 736-keV γ ray were unusual because the singles and coincidence experiments did not agree. In the ^{12}C experiment the intensities derived from the singles and coincidences were 61 and 41 respectively, while in the ^{16}O experiment they were 56 and 42. We found no evidence in the coincidence data or excitation function to indicate that we were seeing a second 736-keV γ ray in another nucleus. Our results are consistent with a state at 736 keV which decays directly to the ground state and thus does not appear in the coincidence data. A weak, low-spin state ($I = \frac{1}{2}$ or $\frac{3}{2}$) at approximately this energy was seen in the ^{102}Pd$(d, t)^{101}$Pd experiment.[8] If such a state is present, its energy cannot differ more than 0.2 keV from 736.2 keV because there was very little if any extra width observed for the 736-keV peak.

Since there is less interference following the α reaction than the C and O reactions, it might appear that the $(\alpha, 2n)$ reaction was the best method of producing ^{101}Pd. However, there is a disadvantage to using the $(\alpha, 2n)$ reaction. A 24-MeV α particle can penetrate the Coulomb barrier of all the high-Z materials which are available for collimators and beam stops. Thus special precautions are required to reduce this source of background radiation and neutrons. One should also be aware that the (α, xn) reaction is much less effective than (heavy ion, xn) reactions for exciting quasirotational bands in some nuclei.[14]

The decay scheme of ^{101}Pd is shown in Fig. 2. We have observed three intense γ-ray cascades which account for more than 80% of the γ-ray intensity that can be associated with ^{101}Pd. The relative intensities illustrated in the decay scheme are for the (^{12}C, $3n$) reaction at 48 MeV. The order of the γ rays in a cascade were established primarily by the intensities seen in the coincidence experiments.

Several features of the coincidence data require comment. There are apparently two γ rays in the $\frac{7}{2}^+$ cascade with an energy approximately equal to 904 keV. We reached this conclusion because there was a 904-keV peak in the 904-keV coincidence spectrum with a normalized area of approximately half the normalized area of the 260, 678, and 878 peaks. It is not possible to determine the precise energy of the 904-keV transition because of the background lines listed in Table I.

There is some uncertainty in the location of the 1074- and 1084-keV transitions. The combined result for all coincidence events between the 1074-keV γ ray and the 972-, 911-, and 891-keV γ rays is 270 ± 150 counts, so its location is probably that given in Fig. 2. Nevertheless, it is possible that the 1074-keV γ ray is a side branch feeding the cascade at some other point above the 2641-keV level. There is less uncertainty in the location of the 1084-keV γ ray. It is in coincidence with all other γ rays in the $\frac{5}{2}^+$ cascade, and the number of 1084–947-keV coincidence events observed (210 ± 84) is substantial.

There are significant differences in the γ-ray yields following the three reactions. Notice in Table I that the top states were observed only with the ^{12}C reaction. The absence of these states following the α-particle reaction is probably due

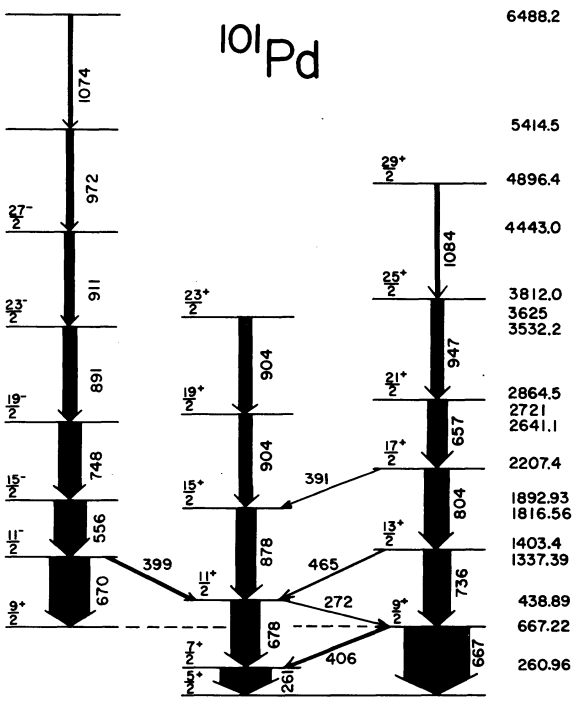

FIG. 2. Decay scheme of ^{101}Pd observed following the reaction ^{92}Zr(^{12}C, $3n$)^{101}Pd using 48-MeV ^{12}C.

to the limited angular momentum brought in. Weak, high-energy γ rays were difficult to observe in the ^{16}O experiment because the ^{88}Sr target was thin. It is also interesting to note that, compared to the ground-state transition, the excited-state cascades were slightly less intense following the α and ^{16}O reactions than they were following the ^{12}C reaction. The 261-keV γ ray was unusually intense following the α reaction, indicating that this reaction was more effective in populating low-lying intrinsic states of the nucleus than ^{12}C or ^{16}O. The $(\alpha, 2n)$ coincidence data were not good enough to locate these states.

The 544-keV γ ray was assigned to ^{102}Rh on the basis of its excitation function as discussed in the preceding section. The coincidence experiment showed that this γ ray was the bottom member of the seven-γ-ray cascade presented in Table II. The intensities are given relative to the 544-keV γ ray (which is only 0.18 as intense as the 677-keV γ ray). The angular distribution coefficients (defined in Sec. III C) are given in columns 4 and 5. The four lower transitions in the cascade are electric quadrupoles while the upper transitions are magnetic dipoles with the possibility of some $E2$ mixture.

The absence of transitions between states in different cascades is important evidence that the cascades are produced by collective excitations built on the band heads. The coincidence data which are pertinent to this question are presented in Table III. Transitions which would be inhibited by angular momentum selection rules were not considered. Instead we looked for cases where $E1$ or $M1$ transitions between cascades could compete with the $E2$ cascade transitions. The first column gives the energy of the initial and final states for the transition being considered. The second column gives the energy the γ ray would have if present. The results given in the third column are the average number of coincident events that were observed when all possible coincidence combinations were considered. For example, the result for the transition from the 2207-

TABLE I. γ rays emitted from ^{101}Pd following (heavy ion, xn) reactions and important background γ rays.

^{101}Pd γ ray Energy (keV)		Intensity of ^{101}Pd γ rays following $(\alpha, 2n)$ at	^{16}O, $3n$ at	^{12}C, $3n$ at	Background γ rays which interfere with ^{101}Pd intensity				
E	ΔE	25 MeV	56 MeV	48 MeV	E	α, xn	^{12}C, xn	Origin	Ref.
260.96	0.05	78	45	77 ±5					
271.67	0.07			2.2 ± 1.4					
390.90	0.07	5		2.4 ± 1.0					
398.56	0.07	2		3.5 ± 1.3					
406.29	0.05	7	5	8.3 ± 1.5					
464.5	0.2	5		3.5 ± 1.4					
					544.2		18	^{102}Rh	text
555.54	0.1	33	26	49 ±4	556.4	17	19	^{102}Pd	1,3
657.07	0.05	9	23	31 ±3					
667.22	0.05	100	100	100	665.3		10	^{100}Pd	1
670.17	0.05	38	41	58 ±5					
677.93	0.05	46	40	45 ±5					
736.2	0.2	44	42	41 ±4					
748.2	0.2	15	20	36 ±4	745.6		23.4	^{98}Ru	4
					750.5		9	^{100}Pd	1
804.02	0.05	21	31	38 ±3					
877.67	0.05	22	22	29 ±3	874.5		2.1	^{98}Ru	4
					875.5		0.8	^{100}Pd	1
891.04	0.1	5	14	22 ±2	892.0		2	^{100}Pd	1
					892.4		1.9	^{102}Pd	1
904.4*A*	1.0	22	18	19 ±5	904.0		7.5	^{98}Ru	4
904.4*B*	1.0			19 ±5	901.7	3	9	^{102}Pd	1,3
910.78	0.1	0	5	15 ±2					
947.47	0.05	8	9	22 ±3	945.4		1	^{100}Pd	1
971.56	0.1	0	0	9 ±1.5	972.0		0.8	^{99}Ru	6
1073.7	0.5	0	0	3.5 ± 1	1073		0.4	^{100}Pd	1
1084.4	0.2	0	0	5 ±1					

keV state to the 1817-keV state was obtained by combining the following coincidence events: the 391-keV γ ray with the 657-, 947-, and 878-keV γ rays; and the 878-keV γ ray with the 657- and 947-keV γ rays. The 947–878-keV coincidence data were included in evaluating the 2208- to 1817-keV transition because we had found that the 2865- to 2721-keV transition was not present.

The multipolarity of the crossing transition is given in column 5. If there is a parity change, the transition is certainly an $E1$. (Potential $M2$ or $E3$ transitions are not included in the table because they would not compete with an $E2$ transition even if the states in the band were not collective.) When there is no parity change the transition is labeled $M1$-$E2$ mixed unless the γ ray was observed in the angular distribution experiment to be primarily $M1$. The experimental branching ratios were calculated using the intensities from Table I and column 4 of Table II. The theoretical branching ratios were taken from Weisskopf single-particle estimates.[15] When the $M1$-$E2$ mixing ratio was not known, the transition was assumed to be $M1$. Since $E1$ transitions generally are much slower than single-particle estimates, a hindrance factor of 10^3 was included in the single-particle estimates for $E1$ γ rays. The comparison of the experimental and theoretical branching ratios clearly shows that the overlap of wave functions is much larger between states in a cascade than for states in different cascades.

C. Angular distributions

The observed angular distribution of the γ rays emitted from a partially aligned nucleus can be expressed in the following form[16]:

$$W(\theta) = 1 + Q_2 A_{22} P_2(\cos\theta) + Q_4 A_{44} P_4(\cos\theta), \qquad (1)$$

where the Q_k are solid-angle correction factors and the P_k are Legendre polynomials. The angular distribution coefficients A_{kk} can be expressed as products of the γ distribution coefficient $A_k(\gamma)$ and the parameters $B_k(I)$ that describe the (axially symmetric) orientation of the nuclear state I:

$$A_{kk} = B_k(I) A_k(\gamma). \qquad (2)$$

For pure multipole radiation, $A_k(\gamma)$ is simply an F coefficient. If only orbital angular momentum is transferred to the nucleus in a reaction and no angular momentum is carried away by emitted particles or γ rays, only $m = 0$ states are populated and

$$B_k^0(I) = (-1)^I (2I+1)^{1/2} \langle I0\, I0 \,|\, k0 \rangle. \qquad (3)$$

In general, the actual $B_k(I)$ are smaller than $B_k^0(I)$ because of neutron emission etc., and an attenuation factor α_k (≤ 1) can be defined by

$$B_k(I) = \alpha_k B_k^0. \qquad (4)$$

For a pure multipole γ transition α_k can be determined from

$$\alpha_k = \frac{A_{kk}(\text{observed})}{B_k^0(I) F_k} \qquad (5)$$

if the spin I of the nuclear states are known. Tables of $B_k^0(I)F_k$ have been prepared by Yamazaki.[16] Once $\alpha_k(I_i)$ is known for a state I_i, $\alpha_k(I_f)$ can be determined for a state I_f which is formed by a pure multipole transition L from the state I_i,

$$\alpha_k(I_f) B_k(I_f) = u_k(I_i\, L I_f)\, \alpha_k(I_i) B_k(I_i). \qquad (6)$$

The deorientation coefficients u_k have also been tabulated.[16] In practice there are usually other transitions which also feed the final state I_f. Nevertheless, the u_k coefficients are still useful to see if the general trend toward deorientation is consistent with theoretical predictions.

A second important consistency check can be made by assuming that the distribution of the initial m-substate population is Gaussian. Then the value of α_k is not very dependent on the angular momentum I_i of the initial state, but rather is primarily determined by the relative width (σ/I_i) of the Gaussian distribution.[3] The correct value of σ is not easy to estimate [except for the special case represented by Eq. (6)], but obviously the same value applies for α_2 and α_4. Curves have been presented[3, 16] which make it easy to check if the observed value of α_2 and α_4 for a transition are consistent—i.e., correspond to a single value of (σ/I_i).

The results of the angular distribution experiments and the analysis outlined above are given in Table IV. The γ rays are listed by their position in the cascades in descending order so that the consistent pattern of deorientation is easy to see. The experimental values of the angular distribution coefficients A_{22} and A_{44} are given in columns 3 and 4. A_{22} and A_{44} were determined

TABLE II. γ rays emitted following the reaction ^{92}Zr(^{12}C,p-n)^{102}Rh. These γ rays are members of a single cascade. The angular distribution parameters A_{22} and A_{44} are defined in Eq. 1.

E	ΔE	Relative intensity	A_{22}	A_{44}	Multipolarity
189.0	0.2	28± 3	−0.155±0.016	−0.007±0.021	$M1(E2)$
305.9	0.3	28± 3	Masked by strong 306.3 keV line in singles		
319.6	0.3	20± 3	−0.142±0.046	+0.118±0.067	$M1$-$E2$
355.21	0.05	86±15	0.323±0.014	−0.094±0.017	$E2$
544.21	0.05	100	0.216±0.018	−0.077±0.026	$E2$
705.4	0.10	75±10	0.402±0.019	−0.160±0.024	$E2$
782.84	0.05	45± 6	0.364±0.038	−0.062±0.046	$E2$

from a least-square fit of Eq. (1) to the experimental data points. The uncertainties were taken as the diagonal elements of the error matrix obtained from the least-square fit. The spin assignments are given in column 5. The angular distribution results by themselves leave an ambiguity in all of the $\Delta I = 2$, $E2$ transition assignments. The experimental results are also consistent with $\Delta I = 0$, $M1$-$E2$ mixed transitions. This ambiguity is removed by the linear polarization measurements which will be presented next, so the $\Delta I = 0$ possibility is not included in Table III. The theoretical values of $B_k^0 F_k$ for pure transitions are given in columns 5 and 6. The procedure for analyzing mixed transitions, where $A_k(\gamma)$ depends on the mixing ratio δ, will be discussed later in this section. The attenuation coefficient α_2' which would be expected if the initial state for the transition were fed only by the preceding transition in the cascade is given in column 7 [see Eq. (6)]. The actual attenuation coefficients [from Eq. (5)] are given in the next two columns. Finally, the last two columns list the range of σ/I values computed from the observed values of α_k under the assumption that the distribution of the m states can be approximated by a Gaussian.

The 5-mg/cm^2 Au backing on the ^{92}Zr target was necessary to reduce Doppler shift distortion of the angular distributions. For example, when the Pd nuclei were permitted to recoil out of the target, the values observed for the 556-keV γ ray were $A_{22} = 0.20 \pm 0.02$ and $A_{44} = -0.10 \pm 0.03$ compared to the results given in Table IV, $A_{22} = 0.322$ and $A_{44} = -0.114$. When the detector was positioned at forward angles, events were lost from a peak if the nucleus was moving when the γ ray was emitted. The loss of counts at forward angles caused A_{22} to appear small and A_{44} to appear large relative to A_{22}.

Even though there was a Au layer on the back of the target, there is still evidence that Doppler shift occurred for γ rays at the top of the cascades. In the $\frac{11}{2}^-$ cascade the lower three γ rays have the angular distributions that one would expect when very little Doppler shift was present. The values of A_{22} and A_{44} are consistent for the 748- and 556-keV transitions; that is, the observed attenuation coefficients α_2 and α_4 correspond to approximately the same value of σ/I. The values of α_2 observed for the 556- and 670-keV transitions are in good agreement with the values of α_2' predicted from the 748- and 556-keV transitions re-

TABLE III. Analysis of coincidence data to investigate crossing transitions between bands in ^{101}Pd. The theoretical values for the cascade-$E2$-to-band-crossing-γ-ray branching ratio were calculated from single-particle estimates with a hindrance factor of 10^3 included for $E1$ transitions. (The seemingly negative numbers are the result of the background subtraction).

E_i	E_f	E_γ	Average coincidence events	Relative intensity	Multipolarity	Branching ratio for E_i $I(E2)/I(C)$ Exp.	Theory
5414.5	4896.4	518.1	−8 ± 18	<0.5	$E1$	>18	0.1
4896.4	4443.0	453.4	−29 ± 21	0.0	$E1$	∞	0.1
4443.0	3812.0	631.0	−14 ± 22	<0.4	$E1$	>38	0.1
3812.0	3625	187	9 ± 10	<1.0	$M1$-$E2$	>22	0.3
3812.0	3532.2	279.8	−26 ± 20	0.0	$E1$	∞	0.1
3625	3532.2	93	−6 ± 8	<0.1	$E1$	>190	20
3532.2	2864.5	667.7	−38 ± 50	<0.6	$E1$	>33	0.1
2864.5	2721	144	−10 ± 5	0.0	$M1$-$E2$	∞	0.06
2864.5	2641.1	223.4	1 ± 15	<0.8	$E1$	>39	0.2
2721	2641.1	80	−4 ± 5	<0.1	$E1$	>190	20
2721	2207.4	514	−31 ± 30	0.0	$M1$-$E2$	∞	0.01
2641.1	2207.4	433.7	8 ± 22	<1.6	$E1$	>22	0.04
2207.4	1892.9	314.5	−12 ± 18	<0.3	$E1$	>127	0.2
2207.4	1816.6	390.8	46 ± 18	2.4 ± 1.0	$M1$-$E2$	16	0.01
1892.9	1816.6	76.3	−4 ± 5	<0.1	$E1$	>490	1
1892.9	1403.4	489.5	25 ± 32	<3.0	$E1$	>16	0.01
1816.6	1403.4	413.2	15 ± 25	<2.1	$M1$-$E2$	>14	0.01
1403.4	1337.4	66.0	8 ± 36	<2.3	$E1$	>18	10
1403.4	938.89	464.5	66 ± 26	3.5 ± 1.4	$M1$-$E2$	12	0.01
1337.39	938.89	398.50	66 ± 25	3.5 ± 1.3	$E1$	17	0.1
938.89	667.22	271.67	41 ± 26	2.2 ± 1.4	$M1$-$E2$	20	0.01
667.22	260.96	406.26	157 ± 28	8.3 ± 1.5	$M1$-$E2$	12	0.01

spectively. One would expect α_2 to decrease going down a cascade because each successive γ ray causes further deorientation of the nucleus. This pattern holds for the 748-, 556-, and 670-keV transitions. Even though one does not expect the Gaussian approximation for the m-state distribution to be perfect, the A_{22} and A_{44} for the 748- and 556-keV transitions show that the approximation is rather good. The observed attenuation coefficients α_2 and α_4 correspond to similar values of σ/I using the assumed Gaussian distribution. Therefore the angular distributions for the 748-, 556-, and 670-keV γ rays are essentially undistorted by Doppler shift, so the average time interval between the formation of the compound nucleus and the emission of the 748-keV γ ray must be longer than the time required for the ^{101}Pd nucleus to slow down in the target or in the Au backing to a velocity where Doppler shift was negligible. An upper limit on the slowing down time of 1 psec was obtained by using range-energy tables.[17]

The 891- and 911-keV γ rays show clear evidence of Doppler shift. Notice that for both of these

TABLE IV. Analysis of angular distributions of γ rays emitted following the reaction ^{92}Zr(^{12}C, $3n$)^{101}Pd using 48-MeV ^{12}C.

E_γ	A_{22}	A_{44}	$I_i \rightarrow I_f$	B_2F_2	B_4F_4	α_2'	α_2	α_4	σ/I from α_2	σ/I from α_4
				$\frac{11}{2}^-$ Cascade						
911	0.220 ± 0.024	−0.13 ± 0.03	$\frac{27}{2} \rightarrow \frac{23}{2}$	0.397	−0.152		0.51–0.61	0.66–1.0	0.37–0.44	0 −0.20
891	0.312 ± 0.016	−0.145 ± 0.025	$\frac{23}{2} \rightarrow \frac{19}{2}$	0.404	−0.161		0.73–0.77	0.74–1.0	0.28–0.30	0 −0.16
748	0.346 ± 0.010	−0.126 ± 0.013	$\frac{19}{2} \rightarrow \frac{15}{2}$	0.414	−0.175		0.81–0.88	0.65–0.79	0.20–0.26	0.15–0.21
556	0.322 ± 0.010	−0.114 ± 0.013	$\frac{15}{2} \rightarrow \frac{11}{2}$	0.429	−0.198	0.78–0.84	0.73–0.78	0.51–0.64	0.28–0.31	0.21–0.26
670	−0.228 ± 0.010	0.008 ± 0.009	$\frac{11}{2} \rightarrow \frac{9}{2}$	−(0.35 → 0.30)		0.69–0.73				
				$\delta = 0 \pm 0.01$						
				$\frac{7}{2}^+$ Cascade						
904	0.278 ± 0.013	−0.109 ± 0.017	$\frac{19}{2} \rightarrow \frac{15}{2}$	~0.41	~−0.17		0.65–0.71	0.54–0.74	0.33–0.36	0.18–0.25
878	0.304 ± 0.013	−0.091 ± 0.014	$\frac{15}{2} \rightarrow \frac{11}{2}$	0.429	−0.198	0.62–0.68	0.68–0.74	0.39–0.53	0.31–0.34	0.25–0.31
678	0.309 ± 0.010	−0.091 ± 0.011	$\frac{11}{2} \rightarrow \frac{7}{2}$	0.455	−0.242	0.64–0.69	0.66–0.70	0.33–0.41	0.33–0.36	0.30–0.33
261	−0.217 ± 0.008	0.013 ± 0.010	$\frac{7}{2} \rightarrow \frac{5}{2}$	−(0.39 → 0.34)		0.58–0.62				
				$\delta = 0 \pm 0.02$						
				$\frac{5}{2}^+$ Cascade						
1084	0.20 ± 0.04	−0.11 ± 0.07	$\frac{29}{2} \rightarrow \frac{25}{2}$	0.394	−0.149		0.41–0.61	0.27–1.0	0.37–0.52	0 −0.35
947	0.295 ± 0.014	−0.054 ± 0.027	$\frac{25}{2} \rightarrow \frac{21}{2}$	0.400	−0.157		0.70–0.77	0.17–0.52	0.28–0.32	0.25–0.42
657	0.343 ± 0.011	−0.121 ± 0.013	$\frac{21}{2} \rightarrow \frac{17}{2}$	0.408	−0.168	0.69–0.76	0.81–0.87	0.64–0.80	0.21–0.25	0.13–0.21
804	0.331 ± 0.010	−0.102 ± 0.011	$\frac{17}{2} \rightarrow \frac{13}{2}$	0.420	−0.185	0.78–0.85	0.77–0.81	0.49–0.61	0.26–0.29	0.23–0.27
736	0.319 ± 0.009	−0.099 ± 0.011	$\frac{13}{2} \rightarrow \frac{9}{2}$	0.440	−0.216	0.73–0.77	0.70–0.75	0.41–0.51	0.31–0.34	0.27–0.30
667	0.309 ± 0.010	−0.091 ± 0.011	$\frac{9}{2} \rightarrow \frac{5}{2}$	0.476	−0.286	0.64–0.69	0.63–0.76	0.28–0.36	0.37–0.39	0.33–0.37
				Crossing transitions						
391	−0.28 ± 0.04	−0.14 ± 0.11	$\frac{17}{2} \rightarrow \frac{15}{2}$	−(0.42 → 0.3)		0.77–0.81				
				$-0.06 \leq \delta \leq 0.02$						
399	0.32 ± 0.03	−0.05 ± 0.05	$\frac{11}{2} \rightarrow \frac{11}{2}$	(0.39 → 0.46)		0.69–0.75				
				$-0.2 \leq \delta \leq 1$						
406	−0.145 ± 0.019	0.06 ± 0.05	$\frac{9}{2} \rightarrow \frac{7}{2}$	−(0.19 → 0.26)		0.63–0.67				
				$0 \leq \delta \leq 0.1$						
465	−0.05 ± 0.03	−0.06 ± 0.06	$\frac{13}{2} \rightarrow \frac{11}{2}$	−(0.03 → 0.11)		0.70–0.75				
				$0.07 \leq \delta \leq 0.3$						

transitions the values of σ/I derived from α_2 and α_4 do *not* agree. Furthermore, α_2 is increasing instead of decreasing for the 911-, 891-, 748-keV γ-ray sequence. These peculiar characteristics occur because A_{22} is small and A_{44} is large for the 911- and 891-keV transitions.

The angular distributions of the 911- and 748-keV γ rays are compared in Fig. 3. The data for the 748-keV γ ray is obviously in excellent agreement with the fitted curve which corresponds to the parameters listed in Table IV. The curve shown with the 911-keV γ-ray data is the result expected if the orientation of the initial state in the 911-keV transition is consistent with the orientation of the initial state in the 748-keV transition. If the additional intensity observed for the 748-keV γ ray is produced by direct feeding of the initial state from the compound nucleus, then the orientation of this state could be more complete than the preceding states. However, in order to account for the large apparent increase in alignment between the 911- and 748-keV transitions, the side feeding would have to come from a relatively low-spin state ($I \lesssim 14$) that was almost completely aligned. Certainly low-spin states are produced in the compound nucleus when the projectile happens to be directed towards the center of the nucleus, but there is no reason to believe that these states would be much more highly aligned after neutron emission than higher-spin states. Even if this preferential alignment hypothesis were correct, it would not explain the lack of consistency between the A_{22} and A_{44} of the 911- and 891-keV γ rays. There is the possibility, however, that our consistency test is not valid if the assumed Gaussian distribution for the m states is a bad approximation for the real distribution. Thus it seems that Doppler shift is the most likely explanation for the observed angular distributions of the 911- and 891-keV γ rays, but other possibilities cannot be excluded.

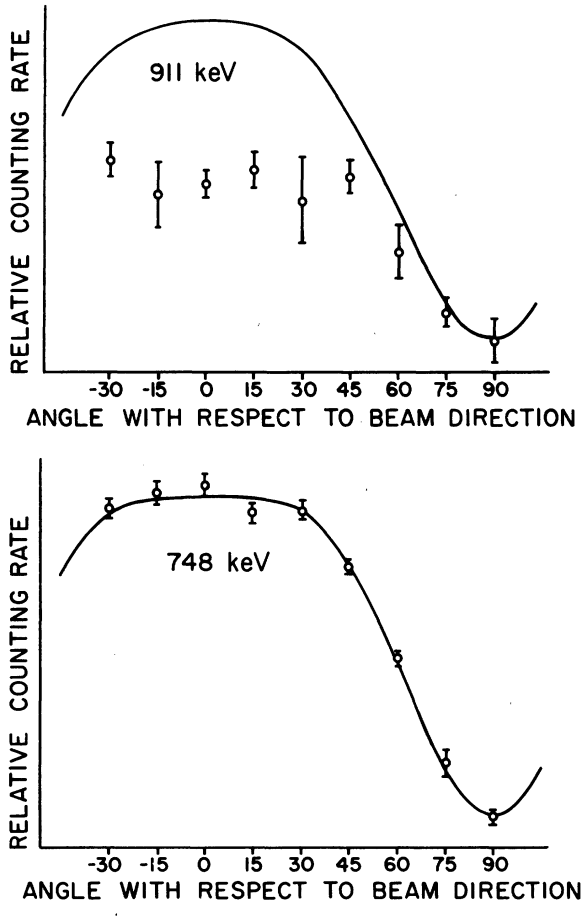

FIG. 3. Comparison of the angular distributions of the 911- and 748-keV γ rays emitted from ^{101}Pd. The large loss in counting rate at forward angles is probably due to doppler shift of the 911-keV γ ray.

We have carefully examined the shape of the 911-keV peak in the γ-ray spectra. There does appear to be a shoulder on the high-energy side of the peak when the spectra taken at forward angles are compared to the spectra taken at 90°. Unfortunately we cannot check for a shoulder on the lower-energy side of the peak at backward angles because of the presence of the more intense 904-keV γ ray. If Doppler shifts were present, as all of the data indicates, the average time between the formation of the compound nucleus and the emission of the 911-keV γ ray must be less than approximately 1 psec.

The same angular distribution patterns are also present in the $\frac{5}{2}^+$ cascade. The angular distributions of the lower four γ rays appear to be essentially undistorted, while the 947- and 1084-keV transitions show evidence of Doppler shift. The α_2 parameters are small for both transitions, particularly the 1084 keV. Again, this is caused by small A_{22}'s. The A_{44} of the 1084-keV γ-ray angular distribution is too large, so the values of α_2 and α_4 do not correspond to the same value of σ/I. Thus it is indicated that the total average time from formation of the compound nucleus to the emission of the 947-keV γ ray is less than approximately 1 psec while the average time to the emission of the 657-keV γ ray is probably greater than this limit. There is much less evidence for Doppler shift in the $\frac{7}{2}^+$ cascade, but this may be because higher-energy states in this cascade were not observed.

The procedure for analyzing transitions which have $\Delta I = \pm 1$ or 0 can be illustrated by considering the 670-keV transition in the $\frac{11}{2}^-$ cascade. The expected attenuation factor α_2' was calculated

from the observed α_2 for the 556-keV transition by using Eq. (6). Then Eq. (5) was used to determine a range of values for $B_2^0F_2$ from A_{22} and α_2'. Once limits on $B_2^0F_2$ were established, the general expression[16] which gives $B_2^0F_2$ for mixed transitions was used to set limits on the mixing ratio

$$\delta = \langle I_f \,|\, L=2 \,|\, I_i \rangle / \langle I_f \,|\, L=1 \,|\, I_i \rangle .$$

In all the mixed transitions A_{44} was predicted to be zero by the extracted mixing ratio. All of the experimental values are consistent with zero with the possible exception of the 391-keV transition which was weak and difficult to measure.

D. γ-ray linear polarization

For a *pure* multipole transition, the linear polarization at 90° to the beam is entirely determined by the angular-distribution coefficients:

$$P_{\text{pure}} = \frac{I(0°) - I(90°)}{I(0°) + I(90°)} = \pm \frac{3A_{22} + 1.25A_{44}}{2 - A_{22} + 0.75A_{44}} \quad \begin{matrix} +\text{no parity change} \\ -\text{parity change} \end{matrix}, \tag{7}$$

where $I(0°)$ and $I(90°)$ are the intensities of the γ rays which have their E vector parallel and perpendicular to the beam direction, respectively (e.g., see Ref. 18). If the transition is of mixed multiple character, the linear polarization P depends also on the spin sequence and the mixing ratio

$$\delta = \langle I_i \,|\, L=2 \,|\, I_f \rangle / \langle I_i \,|\, L=1 \,|\, I_f \rangle .$$

The linear polarization P was measured by observing the relative difference Δ between the counting rates $N(0°)$ and $N(90°)$ for the polarization analyzer crystals parallel and perpendicular to the beam axis, respectively. Since Compton scattering is most probable in a direction perpendicular to the E vector, $N(90°)$ will be greater than $N(0°)$ when P is positive. Thus Δ is defined as

$$\Delta = \frac{N(90°) - N(0°)}{N(90°) + N(0°)}, \tag{8}$$

so the polarization efficiency of the analyzer is a positive number Q defined by the expression

$$Q = \Delta / P. \tag{9}$$

The magnitude of Δ can be used with angular-distribution coefficients to determine the angular-momentum change in a γ transition. Then the sign of Δ determines the electric or magnetic character of the multipole.

The efficiency Q has been calibrated[10] by measuring Δ for γ rays of known polarization P. Q varies from $Q \approx 0.58$ for $E = 250$ keV to $Q \approx 0.31$ for $E = 900$ keV. The measured values of Δ_{exp} and the values expected for a pure transition, Δ_{pure}, are listed in columns 2 and 3 of Table V. Even though there was good agreement between Δ_{exp} and Δ_{pure} for all transitions, an additional test was made to ensure that the assignments were correct. For example, the observed angular distribution of the 667-keV γ ray is consistent with $\frac{9}{2}^+ \rightarrow \frac{5}{2}^+$, pure $E2$, and with a $\frac{5}{2}^+ \rightarrow \frac{5}{2}^+$ mixed $M1 + E2$ transition $1 \leq \delta \leq 2$. The pure $E2$ assignment yields $\Delta_{\text{pure}} = 0.20 \pm 0.04$, in agreement with the experimental value $\Delta_{\text{exp}} = 0.185 \pm 0.012$, whereas the $\frac{5}{2}^+ \rightarrow \frac{5}{2}^+$ assignment yields $-0.06 \leq \Delta_{\text{pure}} \leq -0.02$ in clear disagreement with the experiment. Similar conclusions have been reached for all other transitions assigned as $E2$.

The results obtained for the 670-keV γ transition are particularly interesting. The directional distribution is consistent with an $\frac{11}{2} \rightarrow \frac{9}{2}$ transition that is essentially pure dipole. The polarization data indicates that with this assignment the transition must involve a parity change, i.e., the transition is an essentially pure electric dipole. Several other assignments, all requiring a mixed multipole transition, are consistent with the directional distribution data, but these assignments are at variance with the linear polarization data. Since only the $\frac{11}{2} \rightarrow \frac{9}{2}$ $E1$ assignment is consistent with the data and the $\frac{9}{2}$ state has even parity, the $\frac{11}{2}$ state must have odd parity. Most likely the $h_{11/2}$ orbital is the primary component of the $\frac{11}{2}^-$ state.

The uncertainty in Δ_{pure} is primarily due to the uncertainty in Q. Considering this uncertainty, the angular-distribution results were more effective then the linear polarization measurements in setting limits on the $M1$-$E2$ mixing ratio δ.

TABLE V. Analysis of linear polarization of γ rays emitted following the reaction $^{92}\text{Zr}(^{12}\text{C}, 3n)^{101}\text{Pd}$ using 48-MeV ^{12}C.

E_γ	Δ_{exp}	$\Delta_{\text{pure}} = Q\,P_{\text{pure}}$	Multipolarity
261	−0.159 ± 0.010	−0.16 ± 0.02	$M1$
406	−0.058 ± 0.050	−0.08 ± 0.01	$M1$
556	0.188 ± 0.013	0.22 ± 0.04	$E2$
657	0.191 ± 0.024	0.21 ± 0.04	$E2$
667	0.185 ± 0.012	0.20 ± 0.04	$E2$
670	0.104 ± 0.014	0.11 ± 0.02	$E1$
678	0.169 ± 0.019	0.19 ± 0.04	$E2$
736	0.163 ± 0.016	0.18 ± 0.04	$E2$
748	0.135 ± 0.029	0.19 ± 0.04	$E2$
804	0.200 ± 0.024	0.18 ± 0.04	$E2$
878	0.134 ± 0.027	0.15 ± 0.04	$E2$
891	0.166 ± 0.033	0.15 ± 0.04	$E2$
904	0.118 ± 0.037	0.13 ± 0.03	$E2$
947	0.102 ± 0.035	0.15 ± 0.04	$E2$

IV. DISCUSSION

The results of the coincidence experiments given in Table II clearly show that there is much more overlap between the wave functions of two states within a cascade than there is for two states in different cascades. Thus, it seems quite reasonable to describe the set of states which produce a cascade as members of a "band." The presence of Doppler shift in the angular-distribution experiments indicates that the lifetimes of the upper states in the bands are less than a psec, showing that the states are collective.

How can these collective bands be understood? Nuclei in this mass region have usually been treated as vibrators, and this description may be correct. However, significant static quadrupole moments (~0.5 b) have been observed[19] for the first 2^+ states in ^{106}Pd, ^{108}Pd, and ^{110}Pd, providing evidence that heavier Pd nuclei are deformed. An interpretation[14] of the "threshold effect" which we have reported for ^{101}Pd, ^{103}Pd, and ^{105}Pd suggests that the quasirotational bands in these nuclei involve deformed states. Thus it is attractive to consider the effects of soft deformations in light Pd nuclei.

The permanent deformation must be quite small, as can be seen from the rather large 2^+-0^+ spacings in ^{100}Pd[1] and ^{102}Pd[1,3] (665.3- and 556.4-keV, respectively). If a moment of inertia is calculated for this 2^+-0^+ step in either nucleus, then $(\hbar^2/2\mathcal{I})I(I+1)$ considerably overestimates the energies of higher-spin states. Thus, if these nuclei are deformed they must be rather soft, so that the deformation increases for higher-angular-momentum states. A variable moment-of-inertia (VMI) model has been proposed to incorporate this feature.[5] The VMI model yields an expression for energies in a rotational band:

$$E_I = [I(I+1)/2\mathcal{I}][1 + I(I+1)/4C\mathcal{I}^3],$$

where

$$\mathcal{I} = \mathcal{I}_0/\{1 - [I(I+1)/2C\mathcal{I}^3]\}.$$

The parameter C effectively describes an increase of the moment of inertia over the constant value $\mathcal{I}_0$. The model also gives a simple estimate of the softness σ of the nucleus, or the relative increase in $\mathcal{I}$ with increasing angular momentum:

$$\sigma = [(d\mathcal{I}/dI)/\mathcal{I}]_{I=0} = 1/2C\mathcal{I}_0^3.$$

The appropriateness of the VMI description of ^{100}Pd and ^{102}Pd was investigated by least-squares fitting the ground-state bands of the two nuclei to the VMI formula. (Levels up to 12^+ were included in the fit.) The results are given in Table VI.

The ground-state band of ^{102}Pd was found to be described quite well by the VMI model. The ^{100}Pd fit requires some explanation. The ratio of the energy of the 4^+ state to that of the 2^+ state ($E4/E2$) is 2.127, which is smaller than the lower limit of $E4/E2 = 2.23$ set for positive $\mathcal{I}_0$ and C. The suggestion has been made that negative values of $\mathcal{I}_0$ should be allowed, and that they reflect a spherical band head.[20] The calculated value of $\mathcal{I}$ for higher states remains positive, so that the physical concept of a negative moment of inertia is avoided. Following this prescription a qualitative fit was obtained. (A large uncertainty is inherent in the magnitude of $\mathcal{I}_0$, and hence in the softness parameter σ, when $\mathcal{I}_0$ is so small. The VMI formulation becomes approximately a one-parameter model in this limit. For example, varying $\mathcal{I}_0$ from 1×10^{-4} to 1×10^{-3} has less than a 3% effect on the energy of the 10^+ state.) The extracted value of $\mathcal{I}_0$

TABLE VI. Comparison of quasirotational-band-energy levels in ^{100}Pd, ^{101}Pd, and ^{102}Pd to VMI model calculations.

Nucleus	^{100}Pd		^{101}Pd		^{101}Pd		^{101}Pd		^{102}Pd	
I (Band head)	0^+		$\frac{5}{2}^+$		$\frac{7}{2}^+$		$\frac{11}{2}^-$		0^+	
$\mathcal{I}_0$ ($\times10^{-4}$)	−31.7		−31.6		0.6		9.9		6.42	
C ($\times10^6$)	4.3		4.3		10.2		7.6		6.8	
σ	3.7		3.7		2.3×10^5		66		280	
I(core)	Exp.	Fit	Exp.	Fit	Exp.	Fit	Exp.	Fit	Exp.	Fit
2	665.3	643.7	667.2	644.8	678	672	556	560	556	560
4	1415.5	1328.5	1403.4	1331.3	1556	1503	1304	1293	1275	1271
6	2188.1	2104.7	2207	2107.6	2460	2468	2195	2136	2111	2091
8	2986.3	2956.3	2865	2959.9	3364	3537	3106	3084	3013	3011
10	3867.2	3865.0	3812	3870.1			4078	4113	3992	4007
12	4758.5	4857.3	4896	4874.0			5152	5240	5054	5071
14	5704.7	5872.0								

indicates that ^{100}Pd ($\beta_0 = -3.2\times10^{-3}$) is spherical in its ground state, and that ^{102}Pd ($\beta_0 = 6.8\times10^{-4}$) has a very small equilibrium deformation. For both ^{100}Pd and ^{102}Pd the parameter β has increased to approximately 2.3×10^{-2} at the 12^+ state. It is difficult to relate this parameter to a deformation, but using the same model β_0 was found to be 3.7×10^{-2} for the ground state of ^{168}Er.[5] Thus the VMI model claims that ^{100}Pd and ^{102}Pd have sizable deformations in their high-spin states. This remarkable change can be understood in terms of the large softness parameters extracted for ^{100}Pd and ^{102}Pd (3.7 and 280) compared to that for ^{168}Er (1×10^{-3}). This description of even-even Pd nuclei seems reasonable so let us consider the effects of soft deformations in odd-A nuclei.

Two features of the ^{101}Pd bands are of primary importance; the difference in angular momentum for adjacent states in a band is $\Delta I = 2$ (rather than the $\Delta I = 1$ sequence observed in strongly deformed nuclei), and the energies of levels in the $\frac{5}{2}^+$ ground-state band are similar to those in the ground-state band of ^{100}Pd. This suggests that the spin of the odd particle is unimportant in determining the energies of states in the band; the core dominates. VMI fits to ^{101}Pd bands were performed assuming a $0^+, 2^+, 4^+, \ldots$ spin sequence for each band, effectively ignoring the odd particle. This is in contrast to the approach of Volkov[21] for strongly deformed nuclei where the angular momentum of the band head was included. The results of the VMI fits are given in Table VI.

The fit to the $\frac{5}{2}^+$ band required a negative value of β_0, and in fact yielded parameters almost identical to those for the ^{100}Pd ground-state band. Although the fit to the $\frac{7}{2}^+$ yielded a small positive value of β_0 (6×10^{-5}), the fit is rather poor, and the energies resemble those of the ^{100}Pd band. The fit to the $\frac{11}{2}^-$ band is quite good. The extracted parameters are in fact similar to those for the ^{102}Pd ground-state band, even though the $\frac{11}{2}^-$ state should be nicely described as an $h_{11/2}$ particle coupled to ^{100}Pd. Since the best value of β_0 is larger for the $\frac{11}{2}^-$ band than for the $\frac{5}{2}$ and $\frac{7}{2}$ bands, it is tempting to imply that the core deformation increases slightly due to the presence of the $\frac{11}{2}^-$ particle. Imanishi, Fugiwara, and Nishi[22] have considered deformations in odd Pd nuclei, and have predicted significant changes in the deformation depending on the state occupied by the odd particle. It is interesting that they are successful in reproducing the $\frac{5}{2}^+$ ground-state spin observed for many odd-A nuclei in this mass region when that result was not indicated in many previous calculations.

The success of the VMI description is not so good that it rules out other approaches, yet combined with other facts it indicates that the ^{101}Pd bands may be rotational in nature. The coupling between the odd particle and the core cannot be the one normally observed in deformed nuclei, since the energies in the band depend on R (not I), and the angular-momentum changes are $\Delta I = 2$. Descriptions of this new type of coupling have been approached from two different points of view.

Stephens and his co-workers[23] have suggested that one should begin with the coupling scheme that is used for strongly deformed nuclei. The Hamiltonian contains a term which is proportional to the square of the core angular momentum $\vec{R}$. However, $\vec{R}$ is replaced by the vector difference between the total angular momentum $\vec{I}$ and the angular momentum $\vec{j}$ of the particle, $\vec{R} = \vec{I} - \vec{j}$. This approach introduces a Coriolis term in the Hamiltonian which becomes important as the deformation of the core is decreased. For relatively small deformations, Stephens *et al.*[23] have shown that "decoupled" bands should be observed which have the energy spacing of the core and $\Delta I = 2$. In principle there would be a multiplet of states for each core state, with I varying from $(R + j)$ to $(R - j)$. Since the Coriolis term is very small when R and j are parallel, the energy of the state with $I = (R + j)$ would be primarily determined by the core. Moreover, the states with $I < (R + j)$ would not be easy to observe following a (heavy ion, xn) reaction. The compound nucleus is usually formed with large angular momentum. At a given energy the state with largest I is picked out because in that case the γ ray carries away minimum angular momentum. The states in the multiplet with $I < (R + j)$ would not be seen unless they were appreciably lower in energy. The Coriolis coupling calculation predicts that the states which could be reached by dipole, quadrupole, or even octupole transitions from the spin aligned states have higher, not lower, energy.

The Coriolis interpretation was successful in explaining bands which are built on $\frac{11}{2}^-$ states in a series of La nuclei.[23] However, it may not be applicable to the $\frac{5}{2}^+$ and $\frac{7}{2}^+$ bands seen in ^{101}Pd. The Coriolis term is proportional to $\vec{R}\times\vec{j}$. When j is reduced, the term is less important. Furthermore, one would not expect the $\frac{5}{2}^+$ and $\frac{7}{2}^+$ levels to be as pure as the $\frac{11}{2}^-$ level. (Since the $\frac{11}{2}^-$ state has negative parity it cannot mix with any other single-particle state from the $N = 4$ major shell because they all have common positive parity.) Stephens *et al.* give the impression that the unique parity of the $\frac{11}{2}^-$ state is not an important factor in their calculations. Nevertheless, it should not be assumed that calculations which are successful for high-spin, unique-parity states would be equally successful for low-spin, common-parity

states.

Harris[24] has approached the coupling problem from an opposite point of view. Harris uses a basis in which R and j are good quantum numbers rather than I and j. He then treats the interaction between the particle and the core as a perturbation. Some calculations have been performed by Harris and also by Kleinheinz[25] but only for high-spin, unique-parity states. The results are similar to those of Stephens *et al.*[23] That is, the energy spacing with $\vec{R}$ and $\vec{j}$ aligned is similar to the spacing of states in the core, and the states which have I less than but close to $(R+j)$ lie above the aligned state. We expect that these calculations soon will be extended to the $\frac{5}{2}^+$ and $\frac{7}{2}^+$ bands of ^{101}Pd.

In addition to the collective effects that we have considered, the band-head states are also interesting. In the simple shell model, one would expect the first three states to be (in order of increasing energy) the $d_{5/2}$, $g_{7/2}$, and $h_{11/2}$. Even when a small deformation is present, these states should be dominant components of the low-lying quasiparticle states. Thus it is not surprising that the $\frac{5}{2}^+$ and $\frac{7}{2}^+$ states seen in the ^{102}Pd$(d, t)^{101}$Pd reaction[8] are essentially pure single-particle states. (The occupation of the $h_{11/2}$ orbital is not large enough in ^{102}Pd for the $\frac{11}{2}^-$ state to be seen in ^{101}Pd.) As we have noted previously,[14] the bands probably would not have been observed if the band heads were not rather pure. For example, suppose that the $d_{5/2}$ strength was split among the several low-lying $\frac{5}{2}^+$ states. It is likely that a band would be built on each of these states. Significant mixing would occur between bands because the band heads would have the $d_{5/2}$ orbital in common. There would be many interband transitions, and the intensity available to the bands would be effectively lost in the emission of a very large number of relatively weak γ rays.

Certainly the criterion of single-particle purity should be at least as good in ^{99}Pd as it is in ^{101}Pd. However, it may well be that the ^{98}Pd core is so close to the closed 50-neutron shell that collective rotational excitation is inhibited. We are currently analyzing our ^{99}Pd experiment to investigate these possibilities.

It is quite possible that the most interesting results offered by ^{101}Pd are still undeveloped. It is difficult to determine the exact nature of the ground-state bands which are seen in near-spherical even-even nuclei. Reasonable fits to the bands can usually be obtained with the two-parameter VMI formula. However, this is certainly not a sensitive proof that the shape of the nucleus actually changes as its angular momentum changes.

Perhaps the bands which are seen in ^{101}Pd provide a more sensitive test of the core motion. All of the following features need to be explained: the 657-keV γ ray in the $\frac{5}{2}^+$ band is the only transition which is not in order of increasing energy. The two excited-state bands deviate much more from the core than the ground-state band. The energy of the lowest transition in the $\frac{11}{2}^-$ band is significantly smaller than the energy of the corresponding transition in the other two bands. The VMI fit of the $\frac{11}{2}^-$ band is better than the fit of the core. In fact, the $\frac{11}{2}^-$ band looks more like the ground-state band in ^{102}Pd rather than the band in ^{100}Pd. The top three transitions in the $\frac{7}{2}^+$ band do not show the usual orderly increase in energy. It is reasonable to expect that a description which can interpret some of these observations will also provide important new information about the motion of the core.

The position of the states in the multiplets should be sensitive to the motion of the core and to the core-particle coupling. Even though these states are difficult to observe, as noted earlier in this discussion, there are several ways in which the angular momentum transferred to the compound system can be reduced so that the probability of exciting lower-spin states will be increased. For example, a ^{3}He ion with appropriately low incident energy must strike the target nucleus head on in order to overcome the Coulomb barrier. The angular momentum transferred to the compound system will be small, and yet the excitation energy in the compound system will be high because of the large positive Q value of the (^{3}He, xn) reaction.

Even when the best reaction is used, the most interesting γ rays will still probably be weak so statistical accuracy will be a problem. The coincidence data reported in this paper required 12 hours to obtain. It is difficult to maintain adequate energy resolution with a single counting rate higher than the 15×10^3 counts/sec that we used. Therefore long counting periods, or better yet, a multiple detector array will be needed to make a definitive search for the multiplet states.

---

*Partially supported by the National Science Foundation.

†Current address: Physics Division, Oak Ridge National Laboratory, Oak Ridge, Tennessee.

‡Current address: Physical Science Laboratory, University of Wisconsin, Stoughton, Wisconsin 53589.

[1] G. Scharff-Goldhaber, M. McKeown, A. H. Lumpkin, and W. F. Piel, Jr., Phys. Lett. 44B, 416 (1973).

[2] S. Cochavi, M. McKeown, O. C. Kistner, and G. Scharff-

Goldhaber, J. Phys. (France) 33, No. 8–9, 102 (1972).
[3]P. C. Simms, R. E. Anderson, F. A. Rickey, G. J. Smith, R. M. Steffen, J. R. Tesmer, Phys. Rev. C 7, 1631 (1973).
[4]C. M. Lederer, J. M. Jaklevic, and J. M. Hollander, Nucl. Phys. A169, 449 (1971).
[5]M. A. J. Mariscotti, G. Scharff-Goldhaber, and B. Buck, Phys. Rev. 178, 1864 (1969).
[6]C. M. Lederer, J. M. Jaklevic, and J. M. Hollander, Nucl. Phys. A169, 489 (1971).
[7]P. C. Simms, F. A. Rickey, and J. R. Tesmer, Phys. Rev. Lett. 30, 710 (1973).
[8]F. A. Rickey, R. E. Anderson, and J. R. Tesmer, to be published.
[9]K. A. Hardy, A. Lumpkin, Y. K. Lee, and G. E. Owen, Rev. Sci. Instrum. 42, 482 (1971).
[10]K. A. Hardy, Y. K. Lee, Jin Kim, P. C. Simms, J. A. Grau, G. J. Smith, and F. A. Rickey, to be published.
[11]K. S. Thorne and E. Kashy, Nucl. Phys. 60, 35 (1964).
[12]G. J. Smith, P. C. Simms, F. A. Rickey, J. A. Grau, and J. R. Tesmer, to be published.
[13]J. A. Grau, F. A. Rickey, G. J. Smith, P. C. Simms, and J. R. Tesmer, to be published.
[14]F. A. Rickey and P. C. Simms, Phys. Rev. Lett. 31, 404 (1973).
[15]A. H. Wapstra, G. J. Nijgh, and R. Van Lieshout, *Nuclear Spectroscopy Tables* (North-Holland, Amsterdam, 1959).
[16]T. Yamazaki, Nucl. Data A3, 1 (1967).
[17]L. C. Northcliffe and R. F. Shilling, Nucl. Data A7, 233 (1970).
[18]P. Taras, Can. J. Phys. 49, 328 (1971).
[19]W. R. Lutz, J. A. Thomson, R. P. Scharenberg, and R. D. Larsen, Phys. Rev. C 6, 1385 (1972).
[20]G. Scharff-Goldhaber and A. S. Goldhaber, Phys. Rev. Lett. 24, 1349 (1970).
[21]A. B. Volkov, Phys. Lett. 41B, 1 (1972).
[22]N. Imanishi, I. Fujiwara, and T. Nishi, Nucl. Phys. A205, 531 (1973).
[23]F. S. Stephens, R. M. Diamond, J. R. Leigh, T. Kammuri, and K. Nakai, Phys. Rev. Lett. 29, 438 (1972).
[24]S. M. Harris, private communication.
[25]P. Kleinheinz, private communication.